Supplementary information

Borosilicate glass nanopipette enhanced by synergistic electrostatic interaction and steric hindrance for ultrasensitive electrochemical detection of nanoplastics in environmental water samples

Mengxue Sun[a], Lei Zhang[a], Linsheng Wang[a], Xiaochen Yang[a], Zihan Hao[a], Qun Ma[b], Zhongfeng Gao[a*]

[a] Key Laboratory of Interfacial Reaction & Sensing Analysis in Universities of Shandong, School of Chemistry and Chemical Engineering, University of Jinan, Jinan 250022, P. R. China.

[b] Department of Chemical Engineering, Graduate School of Engineering, Osaka Metropolitan University, Sakai, Osaka 599-8531, Japan.

*Corresponding author

E-mail address: chm_gaozf@ujn.edu.cn (Zhongfeng Gao).

Contents

Reagents

Uniform polystyrene microspheres (100 nm) were purchased from Shanghai Rhawn Technology Development Co., Ltd. APTES (≥98%) was obtained from Beyotime Biotech Inc. Anhydrous ethanol and potassium chloride were supplied by Shanghai Macklin Biochemical Technology Co., Ltd. Borosilicate glass capillaries (outer diameter: 1.0 mm; inner diameter: 0.58 mm; length: 10 cm) were obtained from Sutter Instrument Co.

Apparatus

The glass nanopipettes were fabricated using a P-2000 laser puller (Sutter Instrument Co.). The morphology of the PS nanospheres was characterized using a field-emission scanning electron microscope. The luminescent state of PS nanospheres within the glass nanopores was visualized using a confocal laser scanning microscope. All electrochemical experiments were conducted using a CHI 760D electrochemical workstation (Chenhua Instrument Co., China).

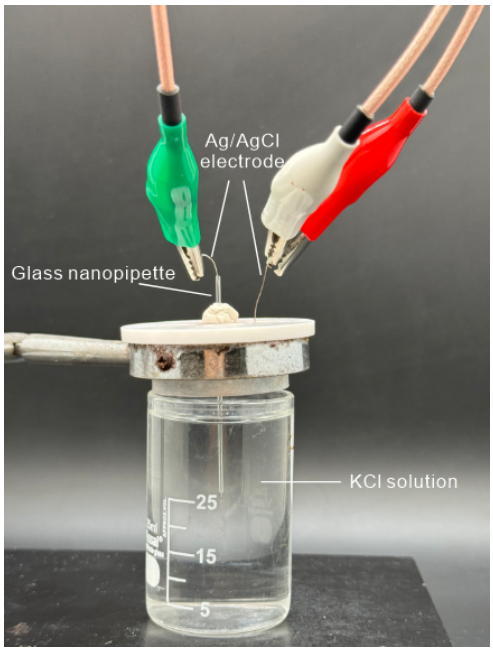

Fig. S1. Schematic diagram of the experimental setup.

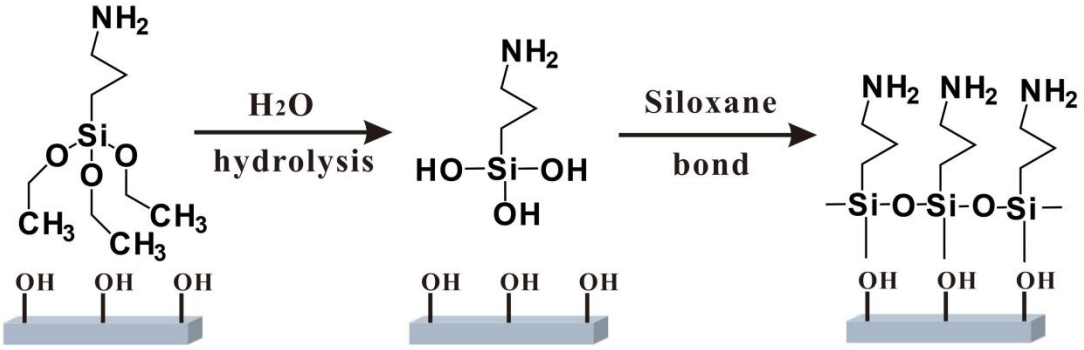

Fig. S2. Covalent immobilization of APTES on a hydroxylated glass surface.

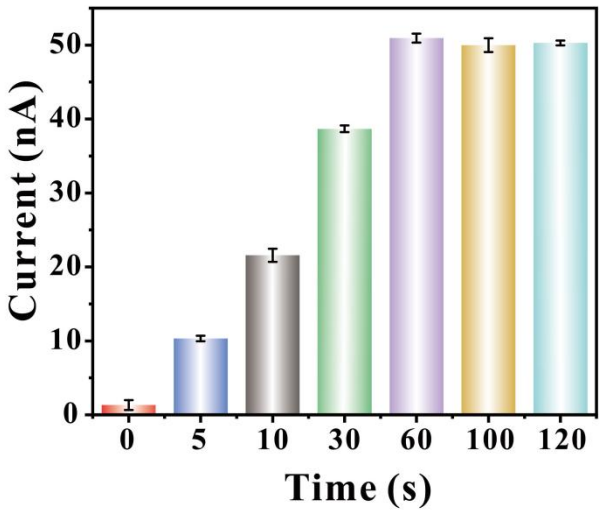

Fig. S3. Optimization of electroosmotic time: Statistical analysis of current signals from APTES-modified nanochannels under +1 V bias at varying electroosmotic durations. Data are presented as mean ± SD (n = 3).

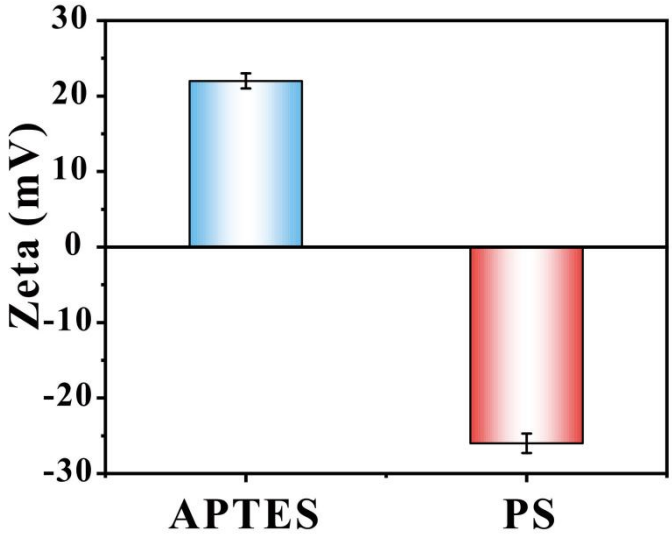

Fig. S4. Zeta potential measurements of APTES and PS nanoplastics, respectively. Data are presented as mean ± SD (n = 3).

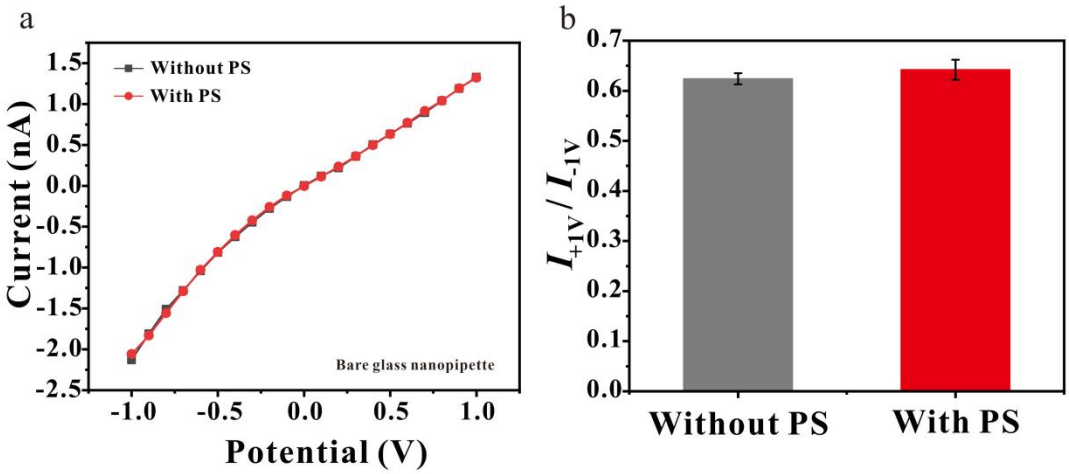

Fig. S5. (a) *I-V* curves and (b) ICR ratios of the bare glass nanopipette before and after interaction with 1 mg/L PS nanoplastics. Data are presented as mean ± SD (n = 3).

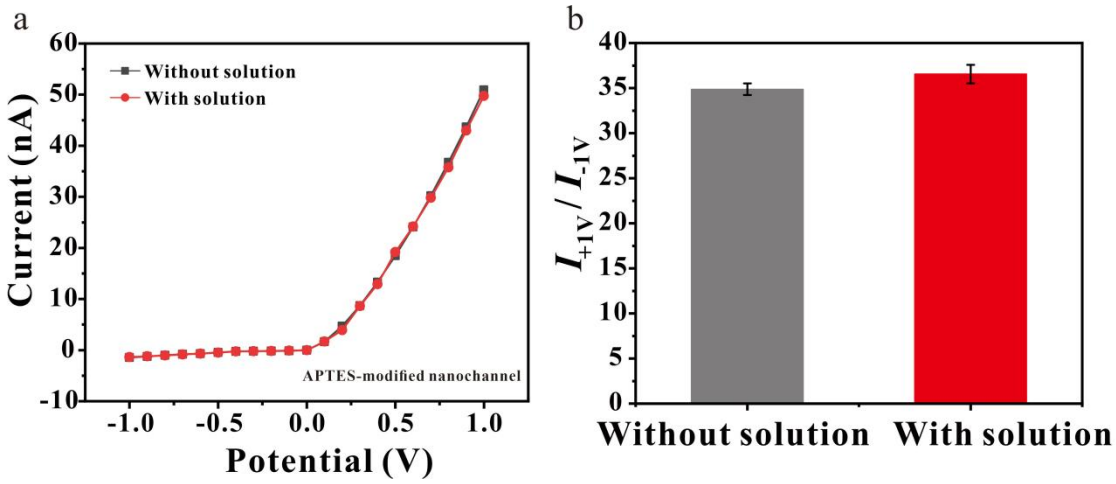

Fig. S6. (a) *I-V* curves and (b) ICR ratios of the APTES-modified nanochannel in PS nanoplastics-free solution. Data are presented as mean ± SD (n = 3).

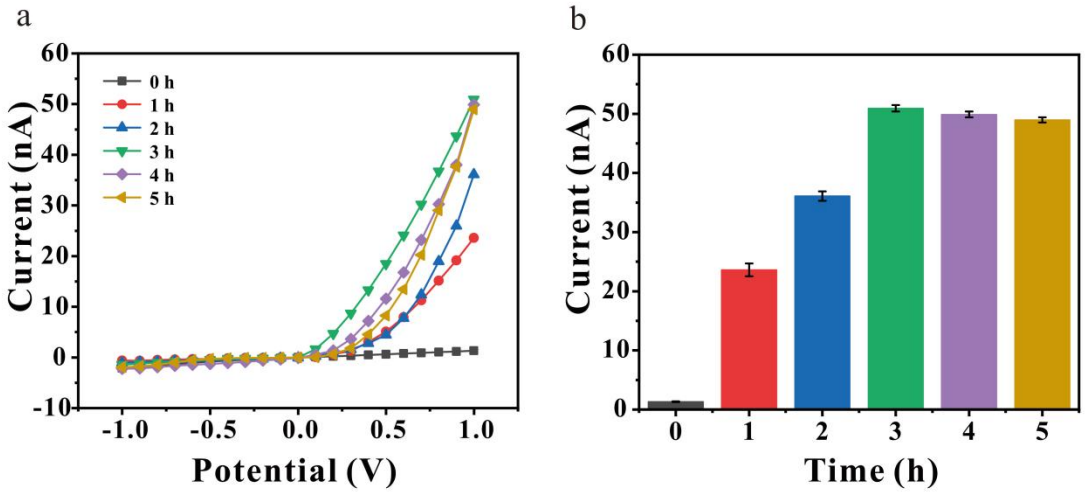

Fig. S7. Optimization of APTES modification time. (a) *I-V* characteristics of nanopipettes at different modification durations. (b) Current signal statistics at +1 V. Data are presented as mean ± standard deviation (n = 3).

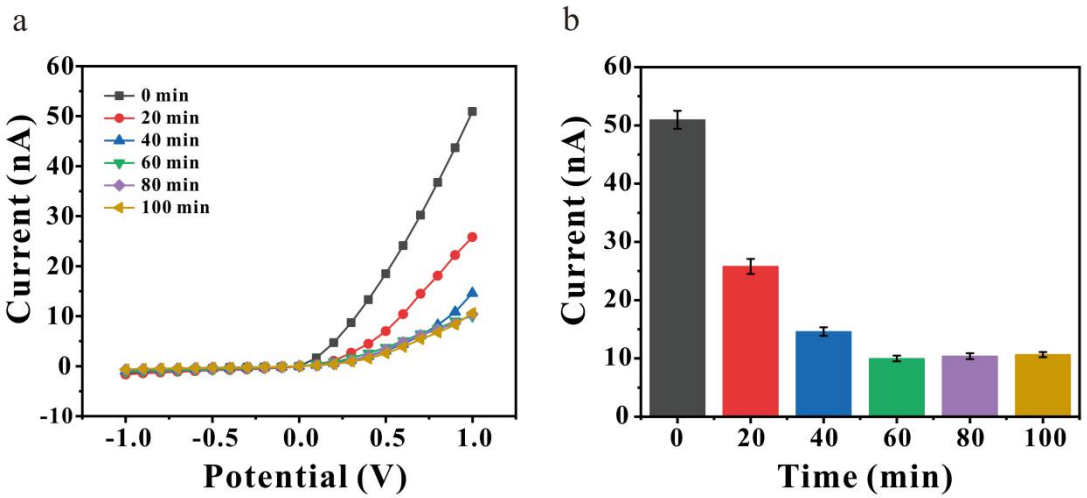

Fig. S8. Optimization of PS nanoplastics exposure time. (a) *I-V* curves of nanopipettes in PS nanoplastics-containing solutions at different exposure durations. (b) Current signal statistics at +1 V. Data represent mean ± standard deviation (n = 3).

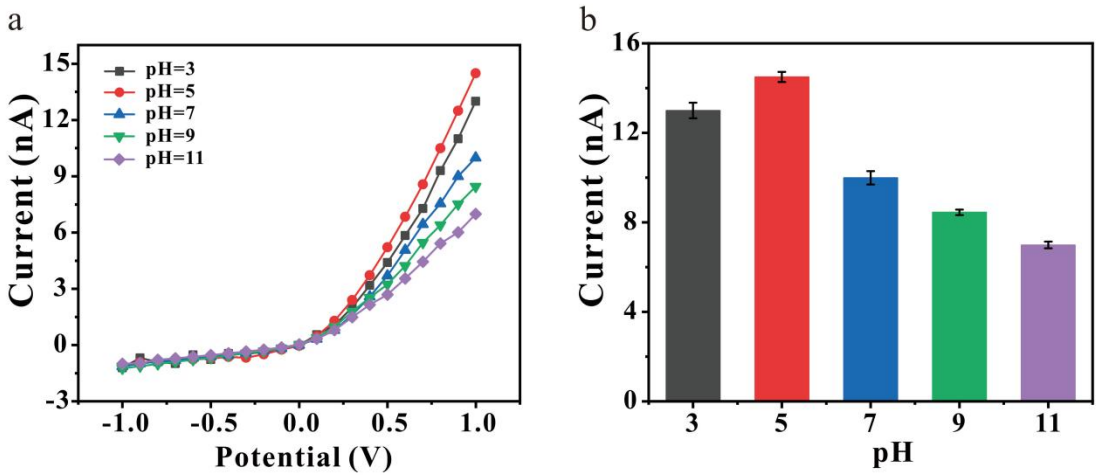

Fig. S9. Optimization of pH in electrolyte solutions. (a) *I-V* characterization of PS nanoplastics-APTES nanopipettes under varying pH conditions. (b) Current signal statistics at +1 V. Data represent mean ± standard deviation (n = 3).

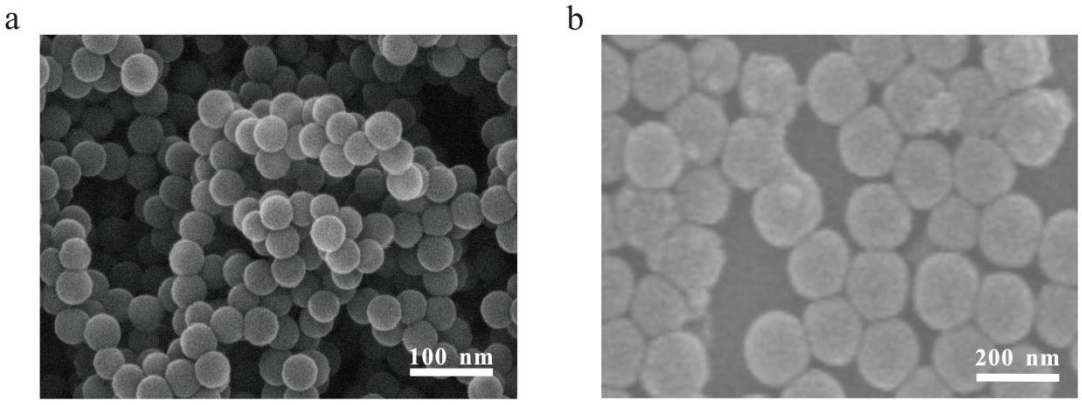

Fig. 10. SEM images of PS nanoplastics: (a) unaged and (b) UV-aged samples.

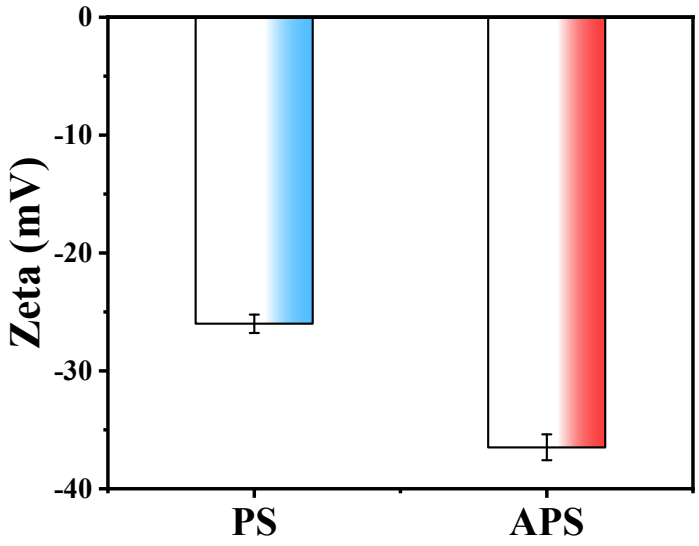

Fig. S11. Zeta potential measurements of pristine PS nanoplastics and aged PS (APS) nanoplastics. Data represent mean ± standard deviation (n = 3).

Table S1. Parameters of the P-2000 laser puller for producing nanopipettes of different sizes.

Dimensions	Parameters	HEAT	FIL	VEL	DEL	PUL
120 nm	1st line value	350	3	30	220	0
	2st line value	340	2	27	180	250
150 nm	1st line value	300	4	33	200	0
	2st line value	290	3	30	160	150
200 nm	1st line value	300	4	28	230	0
	2st line value	290	3	25	200	170
260 nm	1st line value	350	3	30	220	0
	2st line value	350	3	40	180	120

Table S2. Comparison of limit of detection (LOD) for nanoplastics obtained using different methods.

Target	Methods	LOD	References
PS	SERS	10 $mg \cdot L^{-1}$	1
PS	F.L.	0.1-0.3 $mg \cdot L^{-1}$	2
PP	SERS	40 $mg \cdot L^{-1}$	3
PS	Py-GC/MS	2.5-11.5 fM	4
PS	RM	0.05 $mg \cdot g^{-1}$	5
PS	ICP-MS	8.4×10^5 particles$\cdot L^{-1}$	6

Table S3. Determination of PS nanoplastics in two tap water samples.

Sample (μg/L, n = 3)	**Added content** (μg/L, n = 3)	**Detected content** (μg/L, n = 3)	**Recovery** (μg/L, n = 3)
	0	Not detected	/
Sample 1	20.0	19.5	97.5%
	200.0	202.5	101.3%
	0	Not detected	/
Sample 2	20.0	20.3	101.5%
	200.0	198.4	99.2%

Table S4. Determination of PS nanoplastics in spring samples.

Sample (μg/L, n = 3)	**Added content** (μg/L, n = 3)	**Detected content** (μg/L, n = 3)	**Recovery** (μg/L, n = 3)
Heihu Spring	0	11.8	/
	20.0	31.2	97.0%
	200.0	212.3	100.3%
Mo Spring	0	12.5	/
	20.0	32.9	102.0%
	200.0	211.7	99.6%

Notes and references

1. W. Peng, Z.-H. Xu, C. Yi, Y.-K. Zhang and Q.-X. Liao, *Heliyon*, 2024, **10**, e33647.

2. F. Gagné, J. Auclair and B. Quinn, *Environ. Sci. Pollut. Res.*, 2019, **26**, 33524-33531.

3. L.-L. Lv, L. He, S.-Q. Jiang, J.-J. Chen, C.-X. Zhou, J.-H. Qu, Y.-Q. Lu, P.-Z. Hong, S.-L. Sun and C.-Y. Li, *Sci. Total Environ.*, 2020, **728**, 138449.

4. X.-X. Zhou, L.-T. Hao, H.-Y.-Z. Wang, Y.-J. Li and J.-F. Liu, *Anal. Chem.*, 2018, **91**, 1785-1790.

5. Q.-T. Lê, N.-H. Ly, M.-K. Kim, S.-H. Lim, S.-J. Son, K.-D. Zoh and S.-W. Joo, *J. Hazard. Mater.*, 2021, **402**, 123499.

6. J. Jiménez-Lamana, L. Marigliano, J. Allouche, B. Grassl, J. Szpunar and S. Reynaud, *Anal. Chem.*, 2020, **92**, 11664-11672.